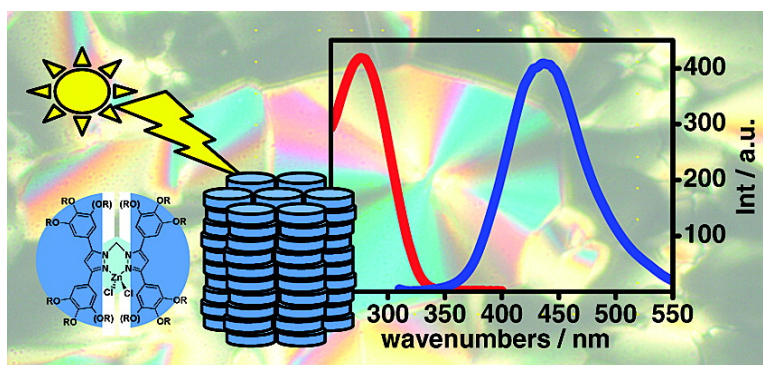


Tetrahedral Zinc Complexes with Liquid Crystalline and Luminescent Properties: Interplay Between Nonconventional Molecular Shapes and Supramolecular Mesomorphic Order

Emma Cavero, Santiago Uriel, Pilar Romero, Jos Luis Serrano, and Raquel Gimnez

J. Am. Chem. Soc., **2007**, 129 (37), 11608-11618 • DOI: 10.1021/ja073639c • Publication Date (Web): 22 August 2007

Downloaded from <http://pubs.acs.org> on February 14, 2009



More About This Article

Additional resources and features associated with this article are available within the HTML version:

- Supporting Information
- Links to the 7 articles that cite this article, as of the time of this article download
- Access to high resolution figures
- Links to articles and content related to this article
- Copyright permission to reproduce figures and/or text from this article

[View the Full Text HTML](#)



ACS Publications
 High quality. High impact.

Tetrahedral Zinc Complexes with Liquid Crystalline and Luminescent Properties: Interplay Between Nonconventional Molecular Shapes and Supramolecular Mesomorphic Order

Emma Cavero,[†] Santiago Uriel,[‡] Pilar Romero,[†] José Luis Serrano,[†] and Raquel Giménez^{*†}

Contribution from the Departamento de Química Orgánica y Química Física, Área de Química Orgánica, Facultad de Ciencias-Instituto de Ciencia de Materiales de Aragón, Universidad de Zaragoza-CSIC, 50009 Zaragoza, Spain, and Centro Politécnico Superior-Instituto de Ciencia de Materiales de Aragón, Universidad de Zaragoza-CSIC, 50015 Zaragoza, Spain

Received May 21, 2007; E-mail: rgimenez@unizar.es

Abstract: Novel metallomesogens with luminescent properties and liquid crystalline behavior at room temperature have been achieved by the preparation of zinc complexes with polycatenar pyrazole and bis-(pyrazolyl)methane ligands. Their molecular structures do not have a conventional shape in that they are far from the typical rod-like and flat disc-like geometries of common liquid crystals. They consist of a nonplanar nucleus due to the methylene spacer and/or the coordination to the tetrahedral center, as confirmed by single crystal analysis of the cores. The different numbers and positions of side chains in the pyrazole ligand enabled us to access lamellar and columnar mesophases and, of particular interest, to obtain columnar arrangements at room temperature. Supramolecular models for the organization of the molecules in the mesophases are proposed on the basis of the small-angle XRD diffractograms. The zinc complexes display luminescence in the near UV-blue region with large Stokes shifts. An interplay between non-conventional molecular shapes (due to the tetrahedral core) and the supramolecular mesomorphic order (due to the ligand design) led to materials that interestingly embody two rather opposite properties, a columnar self-organizational ability and luminescence with weak intermolecular interactions.

Introduction

The study of supramolecular organizations has evolved into a significant topic for the nascent nanotechnologies of molecular electronics and photonics, as it constitutes a starting point for the bottom-up approach to functional materials.^{1–8} Metallomesogens, or metal-containing liquid crystals,^{9–21} offer a viable

approach to multifunctional materials on the basis that they combine the self-organization and self-healing ability of liquid crystals¹⁴ (LCs) with the properties of metal complexes.²² In particular, the combination of luminescence and liquid crystallinity is one possibility that is of relevance for applications in OLEDs, information storage, sensors, and enhanced contrast displays.²³ Luminescent metallomesogens have been reported with metals of the lanthanide group,^{24–29} Pd,^{30–32} Pt,^{33–35} Ni,³⁶

[†] Facultad de Ciencias-Instituto de Ciencia de Materiales de Aragón.

[‡] Centro Politécnico Superior-Instituto de Ciencia de Materiales de Aragón.

- Lehn, J. M. *Rep. Progr. Phys.* **2004**, *67*, 249–265.
- Percec, V.; Glodde, M.; Bera, T. K.; Miura, Y.; Shiyonovskaya, I.; Singer, K. D.; Balagurusamy, V. S. K.; Heiney, P. A.; Schnell, I.; Rapp, A.; Spiess, H. W.; Hudson, S. D.; Duan, H. *Nature* **2002**, *419*, 384–387.
- Liang, C.; Fréchet, J. M. J. *Prog. Pol. Sci.* **2005**, *30*, 385–402.
- Pease, A. R.; Jeppesen, J. O.; Stoddart, J. F.; Luo, Y.; Collier, C. P.; Heath, J. R. *Acc. Chem. Res.* **2001**, *34*, 433–444.
- Amijs, C. H. M.; van Klink, G. P. M.; van Koten, G. *Dalton Trans.* **2006**, 308–327.
- Amabilino, D. B.; Veciana, J. *Supramol. Chirality* **2006**, *265*, 253–302.
- Kato, T.; Mizoshita, N.; Kishimoto, K. *Angew. Chem., Int. Ed.* **2006**, *45*, 38–68.
- Gin, D. L.; Gu, W.; Pindzola, B. A.; Zhou, W.-J. *Acc. Chem. Res.* **2001**, *34*, 973–980.
- Donnio, B.; Guillon, D.; Deschenaux, R.; Bruce, D. W. In *Comprehensive Coordination Chemistry II: From Biology to Nanotechnology*; Mc Cleverty, J. A., Meyer, J. J., Fujita, M., Powell, A., Eds.; Elsevier: Oxford, 2003; Vol. 7, pp 357–627.
- Date, R. W.; Fernández-Iglesias, E.; Rowe, K. E.; Elliott, J. M.; Bruce, D. W. *Dalton Trans.* **2003**, 1914–1931.
- Giménez, R.; Lydon, D. P.; Serrano, J. L. *Curr. Opin. Solid State Mater. Sci.* **2002**, *6*, 527–535.
- Donnio, B.; Bruce, D. W. *Struct. Bonding* **1999**, *95*, 193–247.
- Collinson, S. R.; Bruce, D. W. *Transition Metals in Supramolecular Chemistry*; Wiley: New York, 1999.

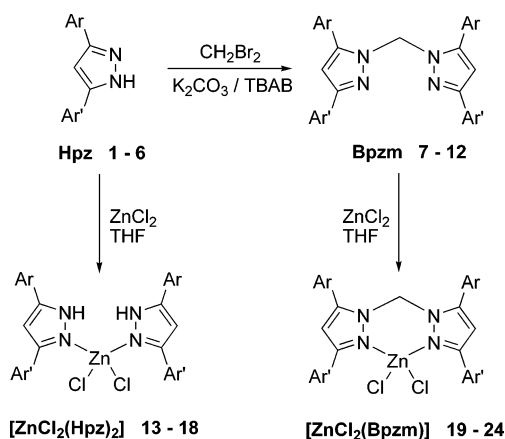
- Handbook of Liquid Crystals*; Demus, D., Goodby, J. W., Gray, G. W., Spiess, H. W., Vill, D. V., Eds.; VCH: Weinheim, 1998.
- Inorganic Materials*; Bruce, D. W., Ed.; John Wiley & Sons: New York, 1997.
- Serrano, J. L. *Metallomesogens: Synthesis, properties and applications*; VCH: Weinheim, 1996.
- Neve, F. *Adv. Mater.* **1996**, *8*, 277–289.
- Hudson, S. A.; Maitlis, P. M. *Chem. Rev.* **1993**, *93*, 861.
- Polishchuk, A. P.; Timofeeva, T. V. *Russ. Chem. Rev.* **1993**, *62*, 291.
- Espinat, P.; Esteruelas, M. A.; Oro, L. A.; Serrano, J. L.; Sola, E. *Coord. Chem. Rev.* **1992**, *117*, 215.
- Giroud-Godquin, A. M.; Maitlis, P. M. *Angew. Chem., Int. Ed.* **1991**, *30*, 375.
- Coe, B. J.; Curati, N. R. M. *Com. Inorg. Chem.* **2004**, *25*, 147–184.
- O'Neill, M.; Kelly, S. M. *Adv. Mater.* **2003**, *15*, 1135–1146.
- Galyametdinov, Y. G.; Haase, W.; Malykhina, L.; Prosvirin, A.; Bikchantaev, I.; Rakhmatullin, A.; Binnemans, K. *Chem.—Eur. J.* **2001**, *7*, 99–105.
- Binnemans, K.; Malykhina, L.; Mironov, V. S.; Haase, W.; Driesen, K.; Van Deun, R.; Fluyt, L.; Gorrler-Walrand, C.; Galyametdinov, Y. G. *ChemPhysChem* **2001**, *2*, 680–683.
- Galyametdinov, Y. G.; Malykhina, L. V.; Haase, W.; Driesen, K.; Binnemans, K. *Liq. Cryst.* **2002**, *29*, 1581–1584.
- Terazzi, E.; Torelli, S.; Bernardinelli, G.; Rivera, J. P.; Benech, J. M.; Bourgogne, C.; Donnio, B.; Guillon, D.; Imbert, D.; Bunzli, J. C. G.; Pinto, A.; Jeannerat, D.; Piguet, C. *J. Am. Chem. Soc.* **2005**, *127*, 888–903.

Au,^{37,38} Cu,³⁹ Ag,^{40,41} and a few examples have concerned their properties in the mesophase. An important example of the interplay between self-organization and luminescence is the recent report of a copper metallomesogen for security ink applications.³⁹

Zinc complexes with nitrogen ligands display interesting optical properties for LED devices and sensors,^{42–47} but the tetrahedral geometry that the metal center usually tends to adopt has proven to be detrimental for mesomorphism. For example, in the extensively studied compounds with salicylaldiminate⁴⁸ or diketonate ligands,¹⁶ complexes derived from Pd, Cu, VO, Ni, Fe, or Mn are LCs but the zinc analogs are not,^{16,49} probably due to the unfavorable geometry and the lack of additional interactions between the metal centers.⁴⁹ Indeed, all previous literature reports on zinc metallomesogens describe the zinc atom in a different coordination geometry, for example, in a planar coordination with porphyrin ligands⁵⁰ and extended analogs, or pentacoordinated with a trigonal-bipyramidal geometry with tris-(2-aminoethyl)amine,⁵¹ dithiobenzoates,⁵² or tridentate pyridines.^{53,54} Therefore, obtaining LC tetrahedral zinc complexes has remained an elusive objective for long time.

We have been investigating pyrazole-based metallomesogens and found that 3,5-diarylpyrazoles are excellent building-blocks for the induction of liquid crystalline behavior at room temperature, as demonstrated by a variety of trinuclear, dinuclear,

Scheme 1



and mononuclear complexes with Au,^{55,56} B,^{57,58} and Rh,⁵⁹ respectively.

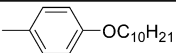
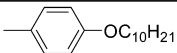
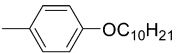
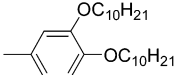
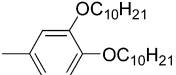
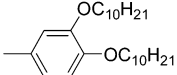
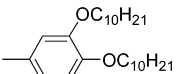
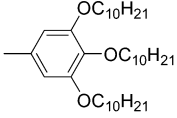
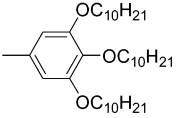
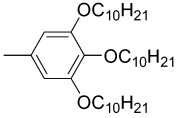
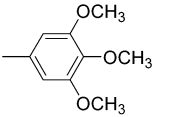
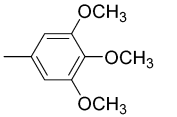
As a result of the versatility of the pyrazole ring, we recently reported that tetrahedral zinc complexes exhibit LC behavior with a flexible ligand design, and we prepared the first liquid crystalline tetrahedral zinc complex by using a nonrigid ligand derived from bis(pyrazolyl)methane.⁶⁰ Afterward, another report on a tetrahedral zinc complex with columnar mesomorphism appeared, and this example contained a nondisoidal dipyridyl ligand.⁶¹

Encouraged by our previous results, we explored new Zn complexes with the aim of obtaining LCs at room temperature and luminescence properties both in solution and in the liquid crystalline state. This objective has been achieved through the preparation of several pyrazoles, Hpz 1–6, which have different numbers (ranging from 2 to 6) and positions of side chains (Scheme 1 and Chart 1), their bis(pyrazolyl)methane derivatives Bpzm 7–12 and their respective Zn complexes of formulas $[\text{ZnCl}_2(\text{Hpz})_2]$ 13–18 and $[\text{ZnCl}_2(\text{Bpzm})]$ 19–24. All of the compounds possess a nonplanar core due to the presence of the methylene spacer and/or coordination to the tetrahedral center. As a result, the molecules do not have a conventional shape in that they are far from the typical rodlike and flat disclike geometries of common LCs. This particular design may have important implications in the optical properties. The synthesis and characterization of the new ligands and complexes, the crystalline structures of complexes 18 and 24, their supramolecular structures in the mesophase, and the optical properties are all discussed. The different numbers and positions of side chains in the pyrazole ligand enabled us to access a variety of mesophases and, in particular, to obtain columnar arrangements with luminescent properties at room temperature. An interplay between nonconventional molecular shapes (due to the tetrahedral core) and the supramolecular mesomorphic order (due to the ligand design) led to materials that combine a

- (28) Suarez, S.; Imbert, D.; Gummy, F.; Piguet, C.; Bunzli, J. C. G. *Chem. Mater.* **2004**, *16*, 3257–3266.
- (29) Yang, Y. T.; Driessen, K.; Nockemann, P.; Van Hecke, K.; Van Meervelt, L.; Binnemans, K. *Chem. Mater.* **2006**, *18*, 3698–3704.
- (30) Neve, F.; Ghedini, M.; Crispini, A. *Chem. Commun.* **1996**, 2463–2464.
- (31) Wen, C.-R.; Wang, Y.-J.; Wang, H.-C.; Sheu, H.-S.; Lee, G.-H.; Lai, C. K. *Chem. Mater.* **2005**, *17*, 1646–1654.
- (32) Ghedini, M.; Pucci, D.; Crispini, A.; Aiello, I.; Barigelletti, F.; Gessi, A.; Franciscangeli, O. *Appl. Organomet. Chem.* **1999**, *13*, 565–581.
- (33) Pucci, D.; Barberio, G.; Crispini, A.; Franciscangeli, O.; Ghedini, M.; La Deda, M. *Eur. J. Inorg. Chem.* **2003**, 3649–3661.
- (34) Damm, C.; Israel, G.; Hegmann, T.; Tschierske, C. *J. Mater. Chem.* **2006**, *16*, 1808–1816.
- (35) Camerel, F.; Ziessel, R.; Donnio, B.; Bourgogne, C.; Guillon, D.; Schmutz, M.; Iacovita, C.; Bucher, J.-P. *Angew. Chem., Int. Ed.* **2007**, *46*, 2659–2662.
- (36) Qi, M.-H.; Liu, G.-F. *J. Mater. Chem.* **2003**, *13*, 2479–2484.
- (37) Bayón, R.; Coco, S.; Espinet, P. *Chem.—Eur. J.* **2005**, *11*, 1079–1085.
- (38) Kishimura, A.; Yamashita, T.; Aida, T. *J. Am. Chem. Soc.* **2005**, *127*, 179–183.
- (39) Kishimura, A.; Yamashita, T.; Yamaguchi, K.; Aida, T. *Nat. Mater.* **2005**, *4*, 546–549.
- (40) Pucci, D.; Barberio, G.; Bellusci, A.; Crispini, A.; La Deda, M.; Ghedini, M.; Szerb, E. D. *Eur. J. Inorg. Chem.* **2005**, 2457–2463.
- (41) Pucci, D.; Barberio, G.; Bellusci, A.; Crispini, A.; Donnio, B.; Giorgini, L.; Ghedini, M.; La Deda, M.; Szerb, E. D. *Chem.—Eur. J.* **2006**, *12*, 6738–6747.
- (42) Kimura, E.; Koike, T. *Chem. Soc. Rev.* **1998**, *27*, 179–184.
- (43) Tanaka, H.; Tokito, S.; Taga, Y.; Okada, A. *J. Mater. Chem.* **1998**, *8*, 1999–2003.
- (44) Jiang, P.; Guo, Z. *Coor. Chem. Rev.* **2004**, *248*, 205–229.
- (45) Miozzo, L.; Papagni, A.; Casalbore-Miceli, G.; Del Buttero, P.; Girotti, C.; Moret, M.; Trabattini, S. *Chem. Mater.* **2004**, *16*, 5124–5132.
- (46) Zuccherro, A. J.; Wilson, J. N.; Bunz, U. H. F. *J. Am. Chem. Soc.* **2006**, *128*, 11872–11881.
- (47) Nolan, E. M.; Ryu, J. W.; Jaworski, J.; Feazell, R. P.; Sheng, M.; Lippard, S. J. *J. Am. Chem. Soc.* **2006**, *128*, 15517–15528.
- (48) Hoshino, N. *Coord. Chem. Rev.* **1998**, *174*, 77–108.
- (49) Pegenau, A.; Hegmann, T.; Tschierske, C.; Diele, S. *Chem.—Eur. J.* **1999**, *5*, 1643–1660.
- (50) Gregg, B. A.; Fox, M. A.; Bard, A. J. *Chem. Commun.* **1987**, 1134–1135.
- (51) Stebani, U.; Lattermann, G.; Wittenberger, M.; Wendorff, J. H. *Angew. Chem., Int. Ed.* **1996**, *35*, 1859.
- (52) Adams, H.; Albeniz, A. C.; Bailey, N. A.; Bruce, D. W.; Cherodian, A. S.; Dhillon, R.; Dunmur, D. A.; Espinet, P.; Feijoo, J. L.; Lalinde, E.; Maitlis, P. M.; Richardson, R. M.; Ungar, G. *J. Mater. Chem.* **1991**, *1*, 843–855.
- (53) Terazzi, E.; Benech, J.-M.; Rivera, J.-P.; Bernardinelli, G.; Donnio, B.; Guillon, D.; Piguet, C. *Dalton Trans.* **2001**, 769–772.
- (54) Morale, F.; Date, R. W.; Guillon, D.; Bruce, D. W.; Finn, R. L.; Wilson, C.; Blake, A. J.; Schröder, M.; Donnio, B. *Chem.—Eur. J.* **2003**, *9*, 2484–2501.

- (55) Barberá, J.; Elduque, A.; Giménez, R.; Oro, L. A.; Serrano, J. L. *Angew. Chem., Int. Ed.* **1996**, *35*, 2832–2835.
- (56) Barberá, J.; Elduque, A.; Giménez, R.; Lahoz, F. J.; López, J. A.; Oro, L. A.; Serrano, J. L. *Inorg. Chem.* **1998**, *37*, 2960–2967.
- (57) Barberá, J.; Giménez, R.; Serrano, J. L. *Adv. Mater.* **1994**, *6*, 470–472.
- (58) Barberá, J.; Giménez, R.; Serrano, J. L. *Chem. Mater.* **2000**, *12*, 481–489.
- (59) Giménez, R.; Elduque, A.; López, J. A.; Barberá, J.; Cavero, E.; Lantero, I.; Oro, L. A.; Serrano, J. L. *Inorg. Chem.* **2006**, *45*, 10363–10370.
- (60) Giménez, R.; Manrique, A. B.; Uriel, S.; Barberá, J.; Serrano, J. L. *Chem. Commun.* **2004**, 2064–2065.
- (61) Barberio, G.; Bellusci, A.; Crispini, A.; Ghedini, M.; Golemme, A.; Prus, P.; Pucci, D. *Eur. J. Inorg. Chem.* **2005**, 181–188.

Chart 1

Ar	Ar'	Hpz	Bpzm	[ZnCl ₂ (Hpz) ₂]	[ZnCl ₂ (Bpzm)]
		1	7	13	19
		2	8	14	20
		3	9	15	21
		4	10	16	22
		5	11	17	23
		6	12	18	24

columnar-ordered organization with weak intermolecular interactions.

Results and Discussion

Synthesis and Characterization in Solution. Polyalkoxy-lated pyrazole ligands Hpz were prepared from 1,3-diketones as reported previously.⁵⁸ These compounds were dimerized to the corresponding bis(pyrazolyl)methanes, Bpzm **7–12**, by reaction with dibromomethane using a solid–liquid phase transfer catalysis method.⁶² The reaction proceeded in a step-wise manner through a 1-(bromomethyl)pyrazole intermediate that reacted with a second molecule of pyrazole. The zinc complexes [ZnCl₂(Hpz)₂] and [ZnCl₂(Bpzm)] were readily prepared by reaction of the Hpz or Bpzm ligands with anhydrous zinc chloride in a 2:1 or 1:1 molar ratio, respectively (Scheme 1).⁶³ All complexes were isolated from the reaction media as white solids or light-yellow greasy materials at room temperature.

1*H*-Pyrazoles display 1,2-prototropy, that is, equilibrium of the NH proton between the two nitrogens, which makes positions 3 and 5 of the heterocycle equivalent on the NMR time scale. Therefore, all pyrazoles, be they symmetrically or unsymmetrically substituted, appear as a single compound. However, when a Bpzm dimer is formed, the 3- and 5-positions of the pyrazole ring become inequivalent and separate signals are observed in the spectra. Similar spectra are also expected for the zinc complexes due to the reduced symmetry. For the full characterization of the new compounds, a careful analysis

was performed on the methoxy-substituted pyrazole **6** and its derivatives (**12**, **18**, and **24**) by ¹H NMR spectroscopy.

The aromatic region of the ¹H NMR spectrum of compound **6** displays a singlet at 6.87 ppm, which corresponds to the four aromatic protons (Figure 1a, H_i, H_e), and another singlet for the proton in position 4 of the pyrazole ring (Figure 1a, H_b). After dimerization takes place to give Bpzm **12**, the spectrum display four singlets, with the signals at 7.04 and 7.31 ppm being due to the aromatic protons located in positions 3 (Figure 1b, H_e) and 5 (Figure 1b, H_i) of the pyrazole ring, respectively. The signals were assigned by means of NOE experiments (see Supporting Information). When compound **12** complexes with zinc to give [ZnCl₂(Bpzm)] **24**, the ¹H NMR spectrum shows four singlets (Figure 1c). Similar NOE experiments were carried out, and it was found that the signal at 7.00 ppm corresponds to the aromatic protons at the 3 position, which is near to the zinc atom, and these remain almost unchanged on complexation (Figure 1c, H_e). However, the protons in the 5-position, which are located far from the metal, are considerably shielded upon coordination (H_i, from 7.31 ppm in Figure 1b to 6.32 ppm in Figure 1c). This unexpected effect is due to the particular conformation of the molecule, as the two aromatic rings in position 5 of the pyrazole rings are very close to one another and are almost parallel, causing a shielding effect due to the anisotropic ring current (see single-crystal X-ray discussion).

On the other hand, the ¹H NMR spectrum of complex [ZnCl₂(Hpz)₂] **18** only shows one signal for the aromatic protons (Figure 1d, H_e, H_i), which is indicative of a high level of symmetry in the compound. This suggests the existence of a 1,2-metallotropic equilibrium in solution, that is, a fast exchange

(62) Diez-Barra, E.; de la Hoz, A.; Sánchez-Migallón, A.; Tejada, J. *Heterocycles* **1992**, *34*, 1365–1373.

(63) Bovio, B.; Cingolani, A.; Pettinari, C.; Lobbria, G. G.; Bonati, F. Z. *Anorg. Allg. Chem.* **1991**, *602*, 169–177.

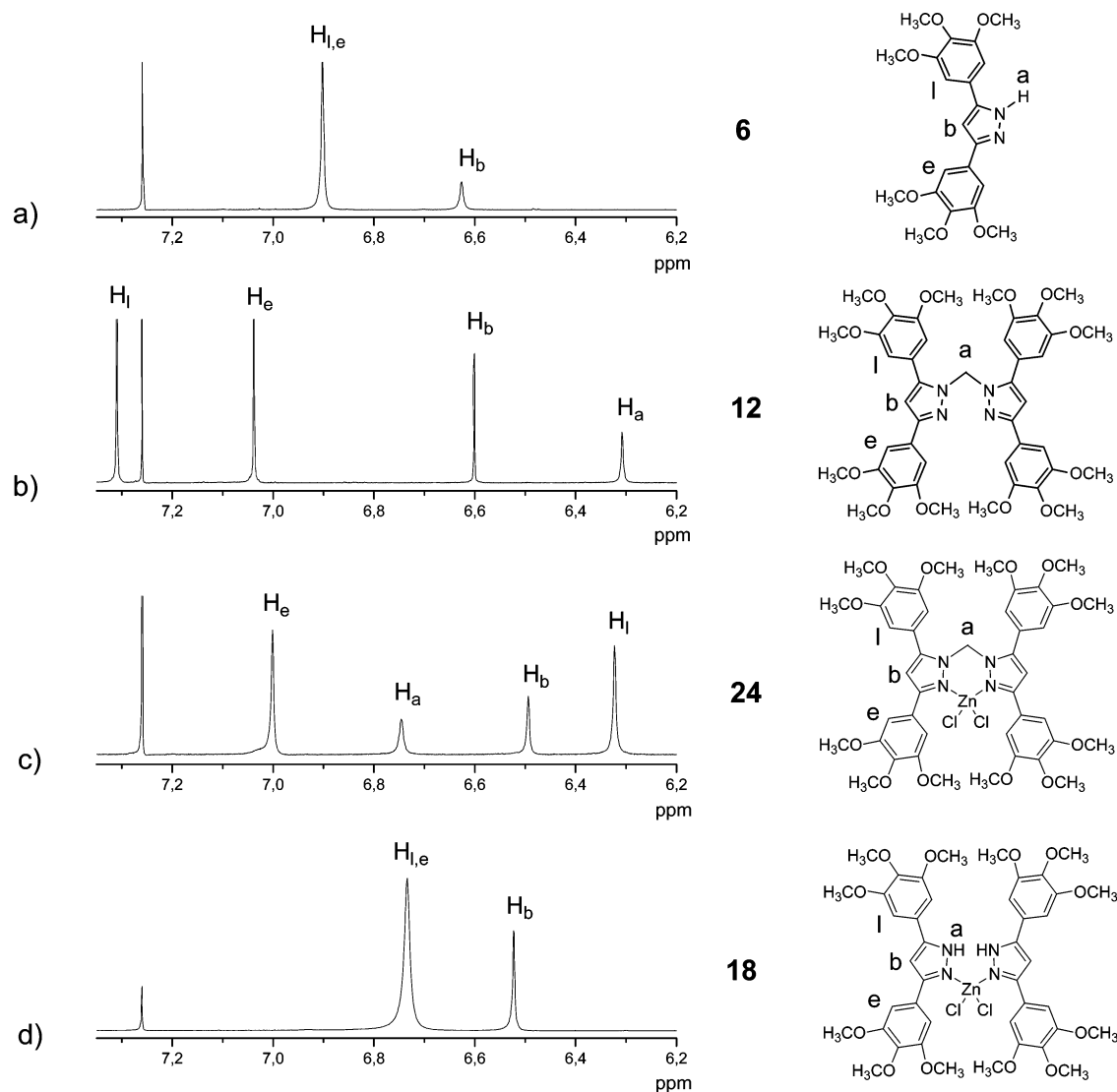


Figure 1. Aromatic region of the ^1H NMR for compound **6** and derivatives **12**, **18**, and **24** in CDCl_3 .

of the Zn atom between the two nitrogens, and this phenomenon has been observed previously in other Rh and Ag complexes with other pyrazole ligands.^{59,64–66} The equilibrium was confirmed by variable temperature ^1H NMR experiments, in which a lowering of the temperature gave rise to splitting of the signals and provides evidence of a reduction in symmetry due to the freezing of the metal interchange.

The proton in the 4-position of the pyrazole (H_b) is almost unchanged upon dimerization (compound **12**) and/or complexation (compounds **18** and **24**), whereas the signals for the protons of the methylene bridge (H_a) are shifted downfield upon complexation (from 6.20 ppm in **12** to 6.80 ppm in **24**).

The above discussion applies to symmetrical decyloxy-substituted Hpzs (**1**, **3**, and **5**) and derivatives. However, more complex spectra were obtained with unsymmetrically substituted Hpzs compounds **2** and **4** due to the presence of regioisomers. In these cases, three possible Bpzms can be obtained, two cis

and one trans (Figure 2). Pyrazoles with small substituents, like 3-methylpyrazole, give rise to the three isomers as a nearly statistical mixture,^{67,68} but in our case, Bpzms **8** and **10** were obtained as a mixture of two regioisomers, one trans and one cis in a 2/1 ratio. Only one of the two possible cis isomers could be identified by COSY, NOESY, and selective 1D-ROESY experiments, and this was identified as the one with fewer alkoxy chains in the 5-position of the pyrazole (Figure 2, cis 1). Therefore, steric effects appear to be of importance in the region close to the methylene bridge and influence the relative proportions of the dimeric isomers obtained. Repeated purification enabled the separation and identification of the trans isomer of compound **8** in its pure form, which helped us to make a full assignment of the NMR signals through COSY and NOE experiments (see Supporting Information).

In the ^1H NMR spectra of the $[\text{ZnCl}_2(\text{Bpzm})]$ complexes **20** and **22**, the signals are broad but the splitting remains unchanged in comparison to that in Bpzm **8** and **10**. Thus, with unsymmetrically substituted ligands, two regioisomers can also be

(64) Gallego, M. L.; Ovejero, P.; Cano, M.; Heras, J. V.; Campo, J. A.; Pinilla, E.; Torres, M. R. *Eur. J. Inorg. Chem.* **2004**, 3089–3098.
 (65) Cano, M.; Heras, J. V.; Maeso, M.; Alvaro, M.; Fernandez, R.; Pinilla, E.; Campo, J. A.; Monge, A. *J. Organomet. Chem.* **1997**, 534, 159–172.
 (66) Cano, M.; Campo, J. A.; Heras, J. V.; Lafuente, J.; Rivas, C.; Pinilla, E. *Polyhedron* **1995**, 14, 1139–1147.

(67) Claramunt, R. M.; Hernández, H.; Elguero, J.; Julia, S. *Bull. Soc. Chim. Fr.* **1983**, 5–10.
 (68) Julia, S.; Sala, P.; Delmazo, J.; Sancho, M.; Ochoa, C.; Elguero, J.; Fayet, J. P.; Vertut, M. C. *J. Heterocycl. Chem.* **1982**, 19, 1141–1145.

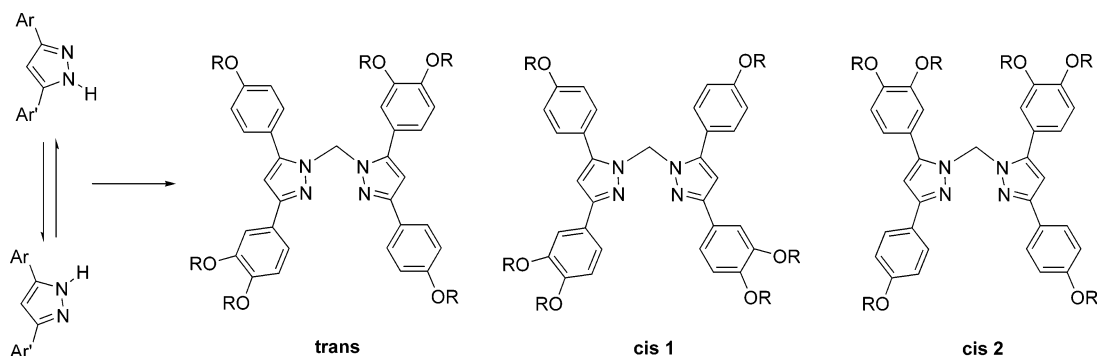


Figure 2. Possible Bpzm isomers derived from unsymmetrically substituted Hpz **2**.

Table 1. Crystal Data and Refinement for Compounds **18** and **24**

compound	18	24
chem formula	C ₄₂ H ₄₈ Cl ₂ N ₄ O ₁₂ Zn·CH ₂ Cl ₂	C ₄₃ H ₄₈ Cl ₂ N ₄ O ₁₂ Zn·3CH ₂ Cl ₂
crystal size/ mm ³	0.27 × 0.23 × 0.08	0.39 × 0.33 × 0.15
crystal system	Triclinic	Triclinic
space group	<i>P</i> $\bar{1}$	<i>P</i> $\bar{1}$
formula weight	1022.04	1203.92
<i>T</i> /K	173(2)	173(2)
θ range data collec /deg	2.72–26.41	2.65–26.39
<i>a</i> /Å	10.8967(4)	10.98830(3)
<i>b</i> /Å	14.5460(7)	13.2389(3)
<i>c</i> /Å	16.0768(9)	18.4296(5)
α /deg	80.091(4)	92.625(2)
β /deg	69.480(4)	99.990(2)
γ /deg	74.809(4)	97.269(2)
<i>Z</i>	2	2
<i>F</i> (000)	1060	1238
<i>V</i> /Å ³	2294.06(19)	2612.83(9)
<i>D</i> _{calc} /gr cm ⁻³	1.48	1.53
μ /mm ⁻¹	0.834	0.943
collected reflns	18149	17658
unique reflns	7673 (<i>R</i> _{int} = 0.0548)	8843 (<i>R</i> _{int} = 0.0223)
restraints/params	0/589	0/696
final <i>R</i> indices [<i>I</i> > 2 σ (<i>I</i>)]	<i>R</i> 1 = 0.0394, w <i>R</i> 2 = 0.0756	<i>R</i> 1 = 0.0305, w <i>R</i> 2 = 0.0724
<i>R</i> indices (all data)	<i>R</i> 1 = 0.0918, w <i>R</i> 2 = 0.0824	<i>R</i> 1 = 0.0456, w <i>R</i> 2 = 0.0760

observed in the same 2/1 ratio. Selective 1D-ROESY experiments confirmed that a conformational effect occurs on complexation, and this leads to shielding of the aromatic protons at the 5-position of the pyrazole ring, as observed with the methoxy compound **24**.

¹H NMR spectra of the [ZnCl₂(Hpz)₂] complexes **14** and **16** display broad signals that are shifted upfield with respect to those in the Hpz ligands, and splitting is not observed. These results suggest the existence of a metallotropic equilibrium in solution, as observed for the methoxy compound **18**.

Single-Crystal Structure of Compounds 18 and 24. The hexamethoxy-substituted complexes **18** and **24** were prepared with the explicit intention of providing further insights into the molecular structure of these new complexes. X-ray quality single crystals were obtained for both compounds by vapor diffusion of hexane into solutions of the compounds in dichloromethane. Data collection and parameters are given in Table 1. ORTEP drawings of the molecular structures with atom numbering schemes and tables containing representative distances and angles are included in the Supporting Information.

Compound **18** crystallizes with a molecule of dichloromethane in the triclinic space group *P* $\bar{1}$, with two formula units per unit cell. The zinc atom is surrounded by two chlorine atoms and two nitrogen atoms in a distorted tetrahedral geometry with a Cl–Zn–Cl angle of 115.7° and an N–Zn–N angle of

119.4°. The largest angular deviation is found for the N–Zn–N angle, a situation in contrast to that found in the structure of [ZnCl₂(dmpz)]⁶⁹ where the Cl–Zn–Cl angle is 119.2° and the N–Zn–N angle is 103.5°. This difference could be due to the structure of the bulky pyrazole ligand. The NH groups of the two pyrazole rings point in opposite directions in a transoid conformation (Figure 3a). The mean planes containing the two pyrazole ligands form an angle of 124°, which gives the compound an overall roof-shape (Figure 3b). The compound is arranged into dimers by a double intermolecular H-bond between the chloro ligand of one molecule and an NH from a pyrazole ring of another molecule situated almost in the same plane (Figure 3c). Both of the NH···Cl distances are ~2.27 Å. In the dimeric structure, only one pyrazole ring of each molecule is involved in an H-bond, being the pyrazole rings not involved in the H-bonding in parallel planes. These dimers are stacked along the *a*-axis (Figure 3d).

Compound **24** also crystallizes in the triclinic space group *P* $\bar{1}$ with two formula units per unit cell. The zinc atom has a distorted tetrahedral coordination with Cl–Zn–Cl and N–Zn–N angles of 114.4 and 95.6°, respectively. The N–Zn–N angle measured for this compound is beyond the upper limit of the values (71–92°) found for other complexes of bis(pyrazolyl)-

(69) Bouwman, E.; Driessen, W. L.; de Graaff, R. A. G.; Reedijk, J. *Acta Cryst.* **1984**, *C40*, 1562–1563.

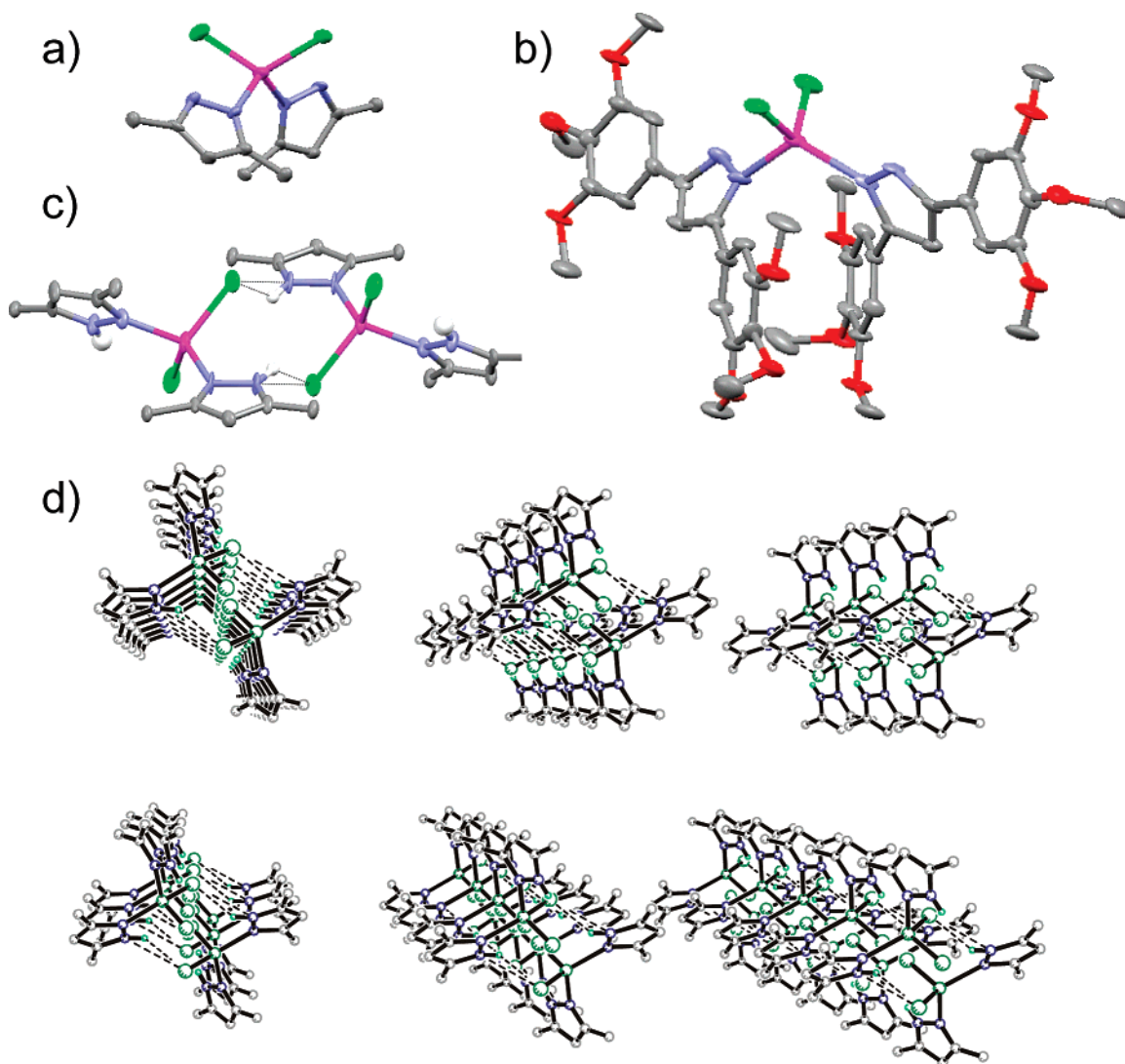


Figure 3. Compound **18**. (a) Detail of the geometry around the metal center, (b) molecular structure, (c) detail of the double intermolecular H-bond, and (d) packing along the *a*-axis (benzene rings and their substituents have been omitted in (a), (c), and (d) for clarity).

alkanes.^{63,70–72} The carbon atom of the methylene bridge is also distorted from the tetrahedral geometry as the N–C–N angle is 112.4°. The central CN₄Zn metallacycle possess a distorted boat conformation in which the carbon atom is the bow and the zinc atom is the stern, situated at angles of 60° (carbon atom) and 10° (zinc atom) with respect to the mean plane formed by the four nitrogens (Figure 1a). The boat shape gives a roof-shaped morphology to the whole molecule, being the fold angle between the mean planes which contain the two pyrazole rings of 132.5° (Figure 4b). The conformation of the metallacycle also forces the aromatic rings situated in the 5-position of the pyrazole rings to arrange closely, at a mean distance of 4 Å in an almost parallel fashion (the mean planes form an angle of ~11°). This conformation probably exists in solution and causes the anisotropic shielding effect of the ring current observed in the ¹H NMR experiments for the aromatic protons in those rings. On the other hand, the presence of the metal atom makes the aromatic rings in the 3-position of the pyrazoles lie further from

each other. Molecular packing along the *b*-axis consists of tilted roof-shaped complexes intercalated by solvent molecules (one ordered and two disordered dichloromethane molecules) and arranged with same boat geometry, which is all-up or all-down (Figure 4c).

Thermal and Mesomorphic Properties. The liquid crystalline properties of the new series of compounds were investigated using polarized light optical microscopy (POM) and differential scanning calorimetry (DSC). Transition temperatures and their associated enthalpy changes are gathered in Table 2.

Pyrazole ligands do not show mesomorphic behavior, except for Hpz **1**, which displays two smectic phases.⁷³ In the Bpzm series, the flexible spacer and the lack of hydrogen bonding gives rise to a considerable lowering of the transition temperatures compared with the pyrazole ligands, and compounds **10** and **11**, with 10 and 12 alkoxy chains, respectively, are liquid crystals and both display a hexagonal columnar phase at room temperature with typical pseudofocal-conic textures.

The zinc complexes [ZnCl₂(Hpz)₂] **13–17** display varied mesomorphism with a gradual change from calamitic to

(70) Bovio, B.; Cingolani, A.; Bonati, F. *Z. Anorg. Allg. Chem.* **1992**, *610*, 151–156.

(71) Pettinari, C.; Cingolani, A.; Bovio, B. *Polyhedron* **1996**, *15*, 115–126.

(72) Pettinari, C.; Marchetti, F.; Cingolani, A.; Leonesi, D.; Colapietro, M.; Margadonna, S. *Polyhedron* **1998**, *17*, 4145–4154.

(73) Barberá, J.; Cativiela, C.; Serrano, J. L.; Zurbano, M. M. *Liq. Cryst.* **1992**, *11*, 887–897.

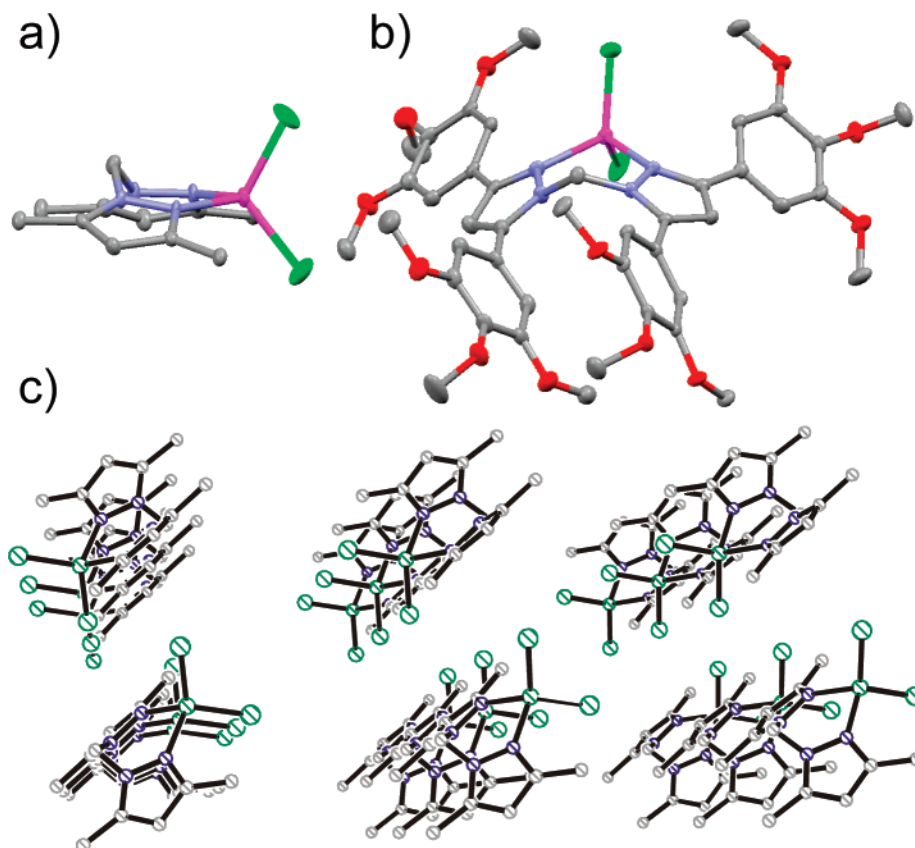


Figure 4. Compound **24**. (a) Boat-shape of the metallacycle, (b) molecular structure, and (c) packing along the *b*-axis (benzene rings and their substituents have been omitted in (a) and (c) for clarity).

columnar mesophases on increasing the number of aliphatic chains, despite the tetrahedral geometry and the low aspect ratio of the molecular structures. In particular, complex **13** (with only 4 decyloxy chains) is not a liquid crystal but, on increasing the number of chains to 6 and 8 (compounds **14** and **15**), the appearance of lamellar mesomorphism was observed with SmA and SmC mesophases. A further increase to 10 chains (compound **16**) led to the disappearance of mesomorphism, and this proved to be the crossover point from lamellar to columnar mesophases because compound **17**, with 12 decyloxy chains, exhibits columnar mesomorphism over a wide thermal range, including room temperature. A marked increase in transition temperatures and extended liquid crystal behavior is observed in these complexes in comparison to the Bpzm series due to the possibility of the ZnCl_2 bridge to interact by additional inter- or intramolecular interactions such as dipolar interactions or H-bonding.^{69,74}

The complexes $[\text{ZnCl}_2(\text{Bpzm})]$ **19–23** display a SmA mesophase (compound **20**) or a columnar mesophase when they bear 6 or more chains (compounds **21–23**). Therefore, for these structures columnar behavior is preferred to lamellar behavior. Zinc complexation of the chelate Bpzm ligands gives a six-membered ring and makes the molecular core more rigid. The fixed structure in these complexes is associated with increases in transition temperatures and stabilities due to a better core/tail microsegregation leading to the arrangement of the molecules in columns.

In both series of Zn complexes, all of the columnar phases gave pseudofocal-conic textures on cooling from the isotropic liquid (Figure 5a). Fan-shaped textures were observed for the

SmA phases (Figure 5b). The SmC phases display an uncharacteristic grainy texture (Figure 5c).

Structural Characterization of the Mesophases. All of the mesomorphic compounds were studied by XRD to confirm the type of mesophase and to study their supramolecular organizations. The observed reflections, proposed indexing, and lattice constants are included in Table 3.

The X-ray diffraction patterns obtained for the SmA phases at high temperatures for complexes **14** and **20**, both of which bear 6 alkoxy chains, contained a diffuse halo corresponding to a mean distance of 4.4 Å. This feature is characteristic of the liquid-like order of the aliphatic chains in a liquid crystal phase. A single sharp reflection was also observed at small angles. The type-A smectic mesophase (SmA) was assigned by textural studies and the small angle reflection was therefore indexed as the first-order reflection of a lamellar mesophase with measured layer spacings of 28.7 and 29.0 Å for compounds **14** and **20**, respectively. These layer spacings are considerably smaller than those measured for the SmA phase of the rod-like pyrazole ligand **1** (34.7 Å)⁷³ and also smaller than for a Zn complex derived from bis(pyrazolyl)ethane (32 Å).⁶⁰ The small value is reasonable if we bear in mind the particular geometry of these molecules as nonplanar and roof-shaped, an arrangement that may leave more free volume to accommodate the conformationally disordered alkyl chains within the layer.

The monotropic nature of the SmC phases of complexes **14** and **15** did not allow us to perform high-temperature experiments. However, we were able to freeze the mesophase at room

(74) Libertini, E.; Yoon, K.; Parkin, G. *Polyhedron* **1993**, *12*, 2539–2542.

Table 2. Phase Behavior of **7–11**, **13–17**, and **19–23**

Compd	Phase ^a	T ^b / °C (ΔH / kJ mol ⁻¹)
7	Cr	$\xrightarrow{129 (59.6)}$ I
8	Cr	$\xrightarrow{70 (81.6)}$ I
9	Cr	$\xrightarrow{62 (162.5)}$ I
10	Col _h	$\xrightarrow{40 (8.0)}$ I
11	Col _h	$\xrightarrow{32^c (10.5)}$ I
13	Cr	$\xrightarrow{108 (95.0)}$ Cr' $\xrightarrow{178 (53.2)}$ I
14	Cr	$\xrightarrow{86^c (25.6)}$ SmC $\xrightarrow{103^c (6.1)}$ SmA $\xrightarrow{80 (1.9)}$ I
		$\xrightarrow{65^c (17.7)}$
15	Cr	$\xrightarrow{82}$ SmC $\xrightarrow{89 (87.9)^d}$ Cr' $\xrightarrow{60 (4.4)}$ I
		$\xrightarrow{46^c (33.1)}$
16	Cr	$\xrightarrow{57^e}$ I
17	Col _h	$\xrightarrow{103^c (4.9)}$ I
19	Cr	$\xrightarrow{97 (16.0)}$ Cr' $\xrightarrow{164 (27.2)}$ I (dec.)
20	Cr	$\xrightarrow{115^c}$ SmA $\xrightarrow{135 (16.3)}$ I
21	Cr	$\xrightarrow{79 (16.0)}$ Col _h $\xrightarrow{112 (2.9)}$ I
22	Col _h	$\xrightarrow{93 (2.8)}$ I
23	Col _h	$\xrightarrow{110^e}$ I

^a Cr, Cr' = crystal, I = isotropic liquid, Col_h = hexagonal columnar, SmA = smectic A, SmC = smectic C. ^b DSC onset peaks. ^c DSC peak maximum. ^d Enthalpy sum of two transitions. ^e POM data.

temperature, and this gave rise to characteristic patterns of smectic mesophases. These patterns showed three sharp maxima in the low-angle region with a reciprocal spacing ratio of 1:2:3. The maxima can be assigned to the (001), (002), and (003) reflections of a lamellar arrangement. The diffuse halo due to the liquid-like arrangement of the aliphatic chains also appeared in these patterns at 4.4 Å. The textural studies, as well as the presence of a SmA phase at higher temperatures in complex **14**, led us to confirm the type-C smectic mesophase (SmC) for the compound. Taking into account the molecular structure for the core provided by the methoxy-substituted complexes and from the powder XRD data, we can propose models for the arrangement of these complexes in the SmA and SmC mesophases, in which roof-shaped molecules arrange in layers (Figure 6). From the X-ray diffraction patterns, it is impossible to extract further information about the arrangement of the molecules within the layers, either as dimeric associations,

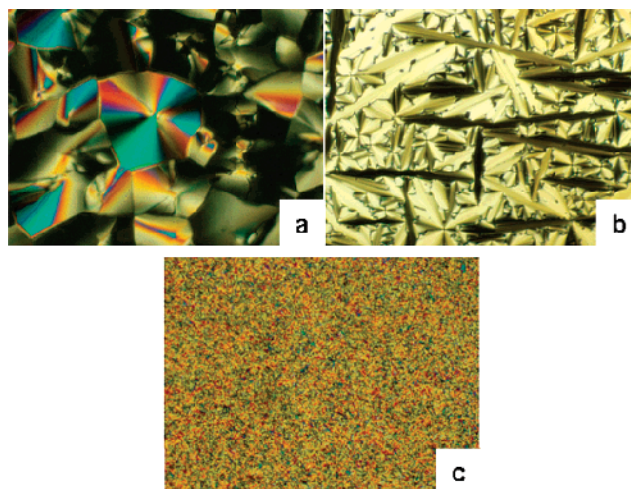


Figure 5. Microphotographs of the textures observed by POM. (a) Columnar phase for **21** at 106 °C. (b) SmA phase for **20** at 123 °C. (c) SmC phase for **14** at 80 °C.

Table 3. X-Ray Diffraction Data for Liquid Crystalline Compounds

compd	phase	T/°C	d-spacing/Å	Miller index/hkl	lattice constant/Å
10	Col _h	r.t.	24.5	100	a = 28.2
11	Col _h	r.t.	25.0	100	a = 28.9
14	SmA	90.0	28.7	001	d = 28.7
	SmC	r.t.	32.2	001	d = 32.2
			14.8	002	
			10.8	003	
15	SmC	r.t.	32.9	001	d = 32.9
			16.5	002	
			11.0	003	
			24.1	100	a = 27.8
17	Col _h	r.t.	14.0	110	
			29.0	001	d = 29.0
			33.6	001	d = 33.6
20	SmA	116	23.9	100	a = 27.5
21	Col _h	90	24.4	100	a = 28.2
	Col _h	r.t.	14.1	110	
			24.2	100	a = 27.9
23	Col _h	r.t.	14.0	110	

as in the crystal structure of **18**, or lateral correlations, as in other folded structures with orthopalladated imines described previously.⁷⁵

The layer spacing of the SmC phase is larger than that of the SmA phase (see XRD data for compound **14**). This difference is due to the loss of conformational freedom at low temperatures, which causes the more extended chains to overcome the effect of tilting (Figure 6a,b).⁷⁶ The same behavior occurs for the SmA phase of compound **20**, where there is a significant increase of the layer spacing on cooling down to room temperature (Figure 6c,d).

With respect to the columnar phases, compounds **10**, **11**, and **21** display typical POM textures and enthalpy values of hexagonal columnar phases, but their X-ray diffraction patterns only show a sharp maximum in the low-angle region and a diffuse halo characteristic of the liquid-like order between the aliphatic chains at 4.4 Å. Although this pattern does not unambiguously confirm the type of mesophase, it rules out other columnar symmetries like rectangular or oblique phases, and it

(75) Espinet, P.; Pérez, J.; Marcos, M.; Ros, M. B.; Serrano, J. L.; Barbera, J.; Levelut, A. M. *Organometallics* **1990**, *9*, 2028–2033.

(76) Baena, M. J.; Barbera, J.; Espinet, P.; Ezcurra, A.; Ros, M. B.; Serrano, J. L. *J. Am. Chem. Soc.* **1994**, *116*, 1899–1906.

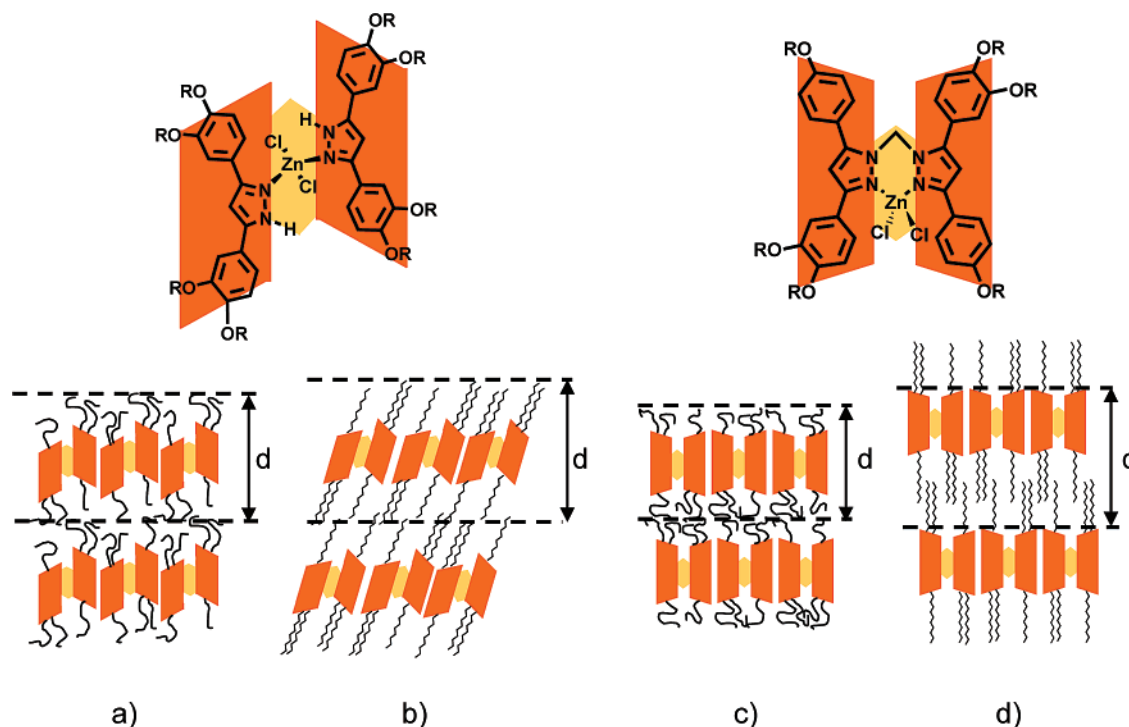


Figure 6. Schematic illustration of the packing modes of the complexes **14** and **20** in the lamellar phases.

has also been found in other structures previously described as hexagonal columnar phases.^{58,77–82} In contrast, complexes **17**, **22**, and **23** yielded diffractograms that are characteristic of hexagonal columnar mesophases. Patterns due to these phases contain a set of two sharp maxima in the low-angle region with a reciprocal spacing ratio of $1:\sqrt{3}$. These maxima can be assigned to the (100) and (110) reflections from the two-dimensional hexagonal lattice. Furthermore, in all three cases, only a diffuse band at 4.4 Å, characteristic of the liquid-like arrangement of the aliphatic chains, was visible in the large angle region, suggesting a poor structural correlation between molecules along the columns.

The supramolecular organization in the columnar mesophase can be analyzed by estimating the number of molecules in a columnar stratum. For this calculation, we take into account the relationship between the columnar cross-section S_{col} , obtained from the a parameter of the hexagonal lattice, and the molecular volume V_m ,⁸³ calculated with the assumption that the density of these compounds in the mesophase at room temperature is $\sim 1 \text{ g cm}^{-3}$. Such a value is acceptable and is commonly used in LCs. From this analysis, we obtain that a single molecule of Bpzm compound **11** occupies the cross-section of one column with a mean stacking distance of 5.3 Å. In the case of the Zn

complexes **17** and **23**, a single complex occupies the cross-section of one column with a larger mean stacking distance, ca. 6.1 Å. As said before, the maximum corresponding to the stacking distance could not be observed in any case in the XRD experiments performed in the mesophase due to the diffuseness together with the failure to obtain oriented patterns, which indicates that the intracolumn order extends only to very short distances. The a parameters of the hexagonal lattice for the zinc complexes are similar; therefore, we exclude the formation of dimers for the $[\text{ZnCl}_2(\text{Hpz})_2]$ complex **17** that could be proposed on the basis of the single-crystal structure of the analogue complex **18**. The lattice parameter is similar to that found for other nonplanar columnar LCs described previously (e.g., pyrazole derivatives),⁵⁸ supporting the conclusion that one single complex occupies the cross section of one column. To ensure a circular spreading of the flexible chains and a loose correlation in the stacking, we propose that the complexes in one column should adopt conformations in which the pyrazole–phenyl torsion angles are different from those observed in the single-crystal structures. The fact that both types of zinc complexes (**17** and **23**) have almost the same lattice parameters despite their different core structures is not surprising if we take into account that they both arrange with one molecule per column stratum, possess similar molecular volumes, and the molten disordered state of the alkyl chains may adopt different conformations around the core. In conclusion, the model proposed for the columnar mesophase involves the stacking of one asymmetric bent-disc molecule in each column for the $[\text{ZnCl}_2(\text{Hpz})_2]$ complex **17** or the stacking of one symmetric bent-disc for $[\text{ZnCl}_2(\text{Bpzm})]$ complexes **21–23** (Figure 7).

Optical Properties. We investigated the optical properties of the Bpzm, $[\text{ZnCl}_2(\text{Hpz})_2]$, and $[\text{ZnCl}_2(\text{Bpzm})]$ series by UV–vis and luminescence spectroscopies in dilute chloroform solutions (Table 4). The spectra of the Bpzm series display a featureless band at around 265 nm, and this corresponds to a

(77) Carfagna, C.; Roviello, A.; Sirigu, A. *Mol. Cryst. Liq. Cryst.* **1985**, *122*, 151–160.

(78) Gramsbergen, E. F.; Hoving, H. J.; Dejeu, W. H.; Praefcke, K.; Kohne, B. *Liq. Cryst.* **1986**, *1*, 397–400.

(79) Mertesdorf, C.; Ringsdorf, H. *Liq. Cryst.* **1989**, *5*, 1757–1772.

(80) Zheng, H. X.; Carroll, P. J.; Swager, T. M. *Liq. Cryst.* **1993**, *14*, 1421–1429.

(81) Barbera, J.; Puig, L.; Serrano, J. L.; Sierra, T. *Chem. Mater.* **2004**, *16*, 3308–3317.

(82) Barbera, J.; Bardaji, M.; Jimenez, J.; Laguna, A.; Martinez, M. P.; Oriol, L.; Serrano, J. L.; Zaragoza, I. *J. Am. Chem. Soc.* **2005**, *127*, 8994–9002.

(83) Both parameters are related by the equation $c S_{\text{col}} = Z V_m$, where c is the stacking periodicity along the columnar axis and Z is the number of molecules within a columnar stratum. For the hexagonal lattice $S_{\text{col}} = \sqrt{3}/2 a^2$. Molecular volume $V_m = M / (0.6023 d)$, where M is the molecular mass and d is the density of the material.

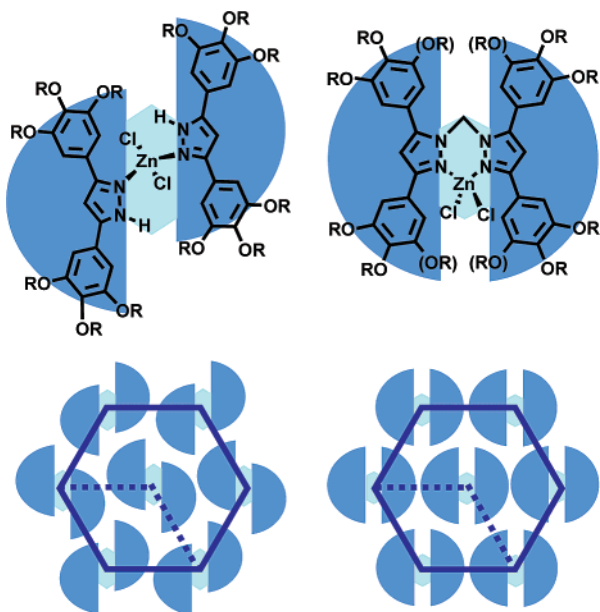


Figure 7. Schematic illustration of the packing mode for **17** (left) and **23** (right) in the columnar phase.

Table 4. Absorption and Emission Data

chain number	compd	$\lambda_{\text{abs}}/\text{nm}$ ($\log \epsilon$)	$\lambda_{\text{em}}^a/\text{nm}$	Stokes shift/ cm^{-1}	I^*/I_{Bpzm}^{*b}
4	7	263 (4.87)	338	8440	1
	13	276 (4.58)	351	7740	6.5
	19	277 (4.79)	367	8850	5.2
6	8	263 (4.82)	347	9200	1
	14	272 (4.77)	384	10700	10.8
	20	277 (4.64)	405	11400	18.7
8	9	265 (4.77)	341	8410	1
	15	270 (4.73)	382	10900	8.4
	21	274 (4.59)	401	11600	12.8
10	10	266 (4.79)	363	10000	1
	16	272 (4.77)	390	11100	2.6
	22	279 (4.61)	419	12000	9.1
12	11	267 (4.80)	385	11500	1
	17	277 (4.74)	412	11800	3.7
	23	277 (4.62)	437	13200	7.5

^a Excited at the absorption maxima. ^b I^* = Intensity of the emission band corrected with the absorption value at λ_{exc} . $I_{\text{Bpzm}}^* = I^*$ of the Bpzm ligand with the same number of chains.

$\pi-\pi^*$ transition. The zinc complexes show a broader and less absorptive band than the Bpzm ligands, with a bathochromic shift of 10–15 nm.

All compounds are luminescent and exhibit an emission band in the near UV-blue region with large Stokes shifts (up to 13 000 cm^{-1}). Excimer emission is excluded as excitation spectra were similar to absorption spectra. In all series, the emission maximum shifts to the red on increasing the number of alkoxy chains. A general trend is also observed if we compare the compounds derived from the same ligand (i.e., with the same number of chains); the emission maxima increase on going from the Bpzm series to the $[\text{ZnCl}_2(\text{Hpz})_2]$ and to the $[\text{ZnCl}_2(\text{Bpzm})]$ series. To estimate the relative emission intensities, we compared the normalized intensities and in all cases found a significant chelation-induced emission enhancement (Table 4). In this respect, the $[\text{ZnCl}_2(\text{Bpzm})]$ chelate complexes are more luminescent (by 5–19 times) than the corresponding Bpzm ligands. In terms of efficiency, we calculated the quantum yield of the compounds with 10 chains to be 0.45% for **10**, 1.3% for **16**,

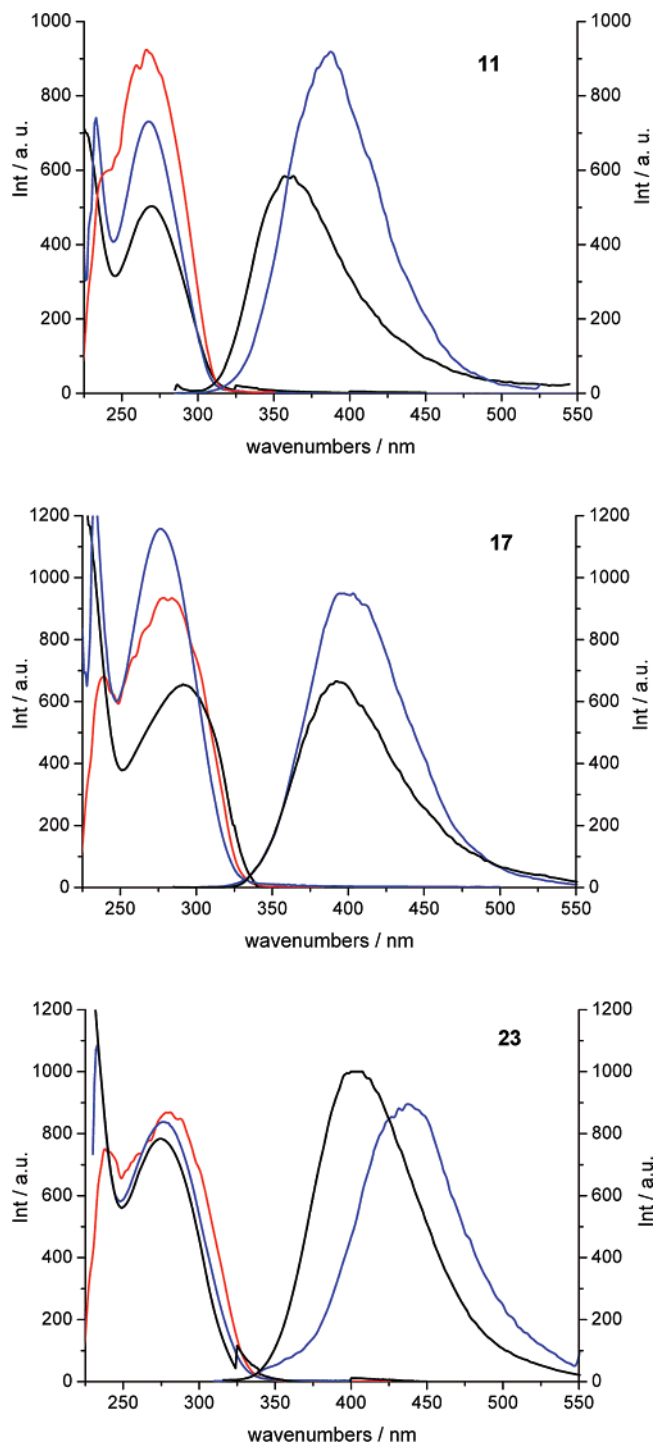


Figure 8. Absorption and emission spectra in dichloromethane solution (blue), absorption and emission in the liquid crystalline state at r.t. (black), and excitation spectra (red) for compounds **11**, **17**, and **23**.

and 5.3% for **22** in dichloromethane solutions with respect to quinine sulfate (54.6% in a 1 N H_2SO_4 solution).⁸⁴ These values follow the same trend as the tabulated normalized emission intensities.

The optical properties of the liquid crystalline compounds **11**, **17**, and **23**, all with 12 decyloxy chains, at room temperature were studied in thin films prepared by pressing the samples between two quartz plates. We found that all three compounds

(84) Eaton, D. F. *J. Photochem. Photobiol. B* **1988**, *2*, 523–531.

are luminescent in the near UV-blue region and exhibit a similar trend in emission and intensities to the solution experiments, where **23** is the compound with the highest emission wavelength (Figure 8). By comparing solution and liquid crystalline state spectra, we observe that compound **17** displays the same emission wavelength both in solution and in solid state, whereas an unexpected blue-shift was observed for **11** (26 nm) and **23** (33 nm). A blue-shift of the fluorescence maximum has been observed previously in the columnar mesophase of intrinsically luminescent liquid crystals when studying the compounds in different phases and has been associated with a decrease in the degree of disorder along the column and a reduction in the ability of the molecules to form self-quenching aggregates.⁸⁵ On the other hand, the design of tetrahedral or globular molecules has proved to be a good synthetic strategy to prevent interchromophore contacts that lead to aggregation or excimer formation, red-shift of the emission bands, and quenching.⁸⁶ In our case, the nonplanar shape of the compounds and the supramolecular organization proposed within the column (see previous section) prevent intracolumnar correlation of the mesogenic cores and could explain why there is no red-shift of the emission band with respect to solutions.

Because the Stokes shift is usually dependent on the structural relaxation of the excited state, the large values found in solution may result from a significant conformational change that occurs upon excitation. Structural changes are sensitive to their microenvironment; therefore, in the liquid crystalline state, the possible different conformation from solution, viscosity, and local order affect the internal rotations leading to a blue-shift in the emission maxima. This effect would be more important for compounds **11** and **23** than for **17**, according to the spectral changes observed. More comprehensive studies are needed to evaluate the mechanisms of this behavior as the compounds may act as intrinsic viscosity probes via internal rotations. Therefore, these liquid crystalline tetrahedral zinc complexes show attractive photophysical properties that make them inter-

esting subjects for future studies in their own right. Furthermore, mesomorphic glassy films of these materials may provide an approach to noncrystalline but organized films of pure compounds with luminescent properties without close intermolecular contacts. Such systems could be useful for the design of novel functional assemblies.

Conclusions

We have developed a synthetic strategy for the preparation of luminescent tetrahedral zinc complexes that show liquid crystal phases at room temperature. The synthetic route involves complexation of zinc(II) chloride to Hpz and Bpzm ligands. These compounds exemplify the delicate balance that leads to liquid crystals in which there is an interplay between an unfavorable tetrahedral core with a low aspect ratio and supramolecular lamellar or columnar order. Luminescent properties have been found in the near UV-blue region and these are associated with large Stokes shifts. The special molecular geometry is also responsible for the optical properties in the mesophase. In this respect, the loose yet ordered columnar packing of luminescent molecules gives rise to emissive pure thin films without appreciable formation of aggregates. The photophysical properties and the potential for optoelectronic applications and UV sensors are open lines to be explored in the near future.

Acknowledgment. We thank the Ministerio de Educación y Ciencia and FEDER, projects MAT2003-07806-C02-01, MAT-2006-13571-CO2-01, the Ramón y Cajal (R.G.) and FPU (E.C.) programs, and the Gobierno de Aragón for financial support.

Supporting Information Available: Full synthetic and analytical details for all new compounds. 1D-ROESY spectra for **12**. ¹H NMR spectra for the characterization of isomers in **8** and **20**. Variable temperature ¹H NMR spectra for **18**. ORTEP molecular drawings with atom numbering scheme and representative distances for **18** and **24**. Crystallographic information files (CIF) for **18** and **24**. This material is available free of charge via the Internet at <http://pubs.acs.org>.

JA073639C

(85) Levitsky, I. A.; Kishikawa, K.; Eichhorn, S. H.; Swager, T. M. *J. Am. Chem. Soc.* **2000**, *122*, 2474–2479.

(86) Wang, S.; Oldham, W. J. J.; Hudack, R. A. J.; Bazan, G. C. *J. Am. Chem. Soc.* **2000**, *122*, 5695–5709.